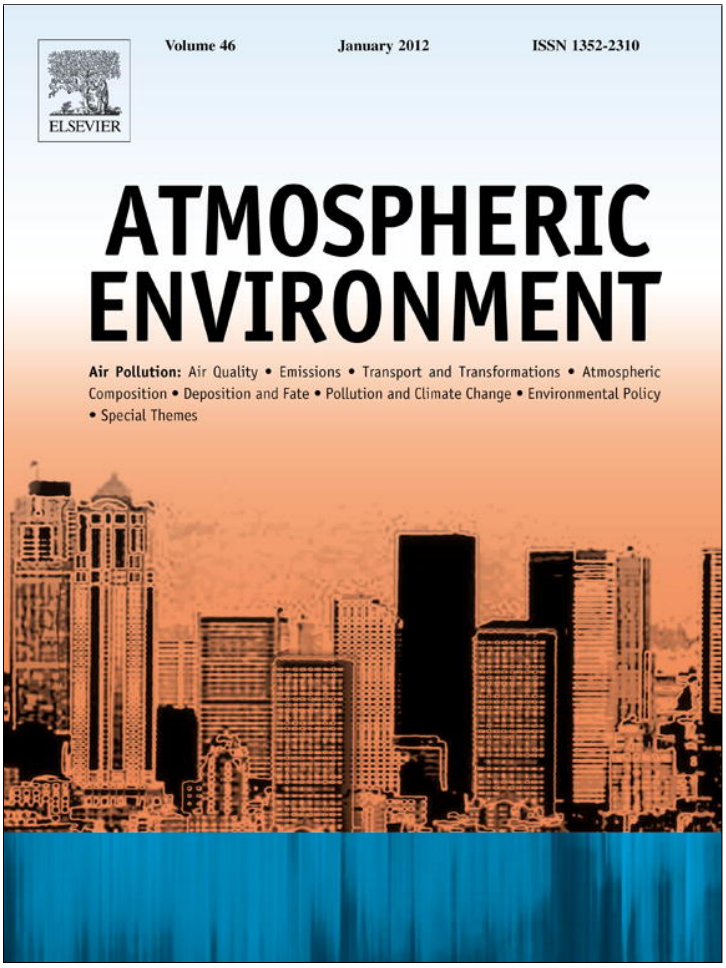
Volume 46
January 2012
ISSN 1352-2310
ELSEVIER
ATMOSPHERIC ENVIRONMENT
Air Pollution: Air Quality • Emissions • Transport and Transformations • Atmospheric Composition • Deposition and Fate • Pollution and Climate Change • Environmental Policy • Special Themes

Atmospheric Environment 71 (2013) 304–310

Contents lists available at SciVerse ScienceDirect

Atmospheric Environment

journal homepage: www.elsevier.com/locate/atmosenv

Short communication

A short-term predictor of satellite-observed fire activity in the North American boreal forest: Toward improving the prediction of smoke emissions

David Peterson [a,*], Edward Hyer [b], Jun Wang [a]

[a] University of Nebraska – Lincoln, Department of Earth and Atmospheric Sciences, Lincoln, NE 68588, USA
[b] Naval Research Laboratory, 7 Grace Hopper Avenue, Monterey, CA 93940, USA

HIGHLIGHTS

► Statistical model predicts daily growth or decay of satellite-observed fires in central Alaska.
► Inputs include MODIS and GOES fire data and NWP-calculated fire weather indices.
► Reduces RMSE compared to a persistence forecast used by smoke emission inventories.
► Improvements are strongest for cases with observed decay or extinction of fires.
► Critical step toward improving operational smoke emission and transport forecasts.

ARTICLE INFO

Article history:
Received 30 July 2012
Received in revised form
26 December 2012
Accepted 28 January 2013

Keywords:
Fire weather
Numerical weather prediction
Satellite
Boreal
Wildfire
Smoke
Emissions
Statistics

ABSTRACT

A statistical model, based on numerical weather prediction (NWP), is developed to predict the subsequent day's satellite observations of fire activity in the North American boreal forest during the fire season (24-h forecast). In conjunction with the six components of the Canadian Forest Fire Danger Rating System and other NWP outputs, fire data from the MODerate Resolution Imaging Spectroradiometer (MODIS) and the Geostationary Operational Environmental Satellites (GOES) are used to examine the meteorological separability between the largest fire growth and decay events, with a focus on central Alaska during the large fire season of 2004. This combined information is analyzed in three steps including a maximum likelihood classification, multiple regression, and empirical correction, from which the meteorological effects on fire growth and decay are statistically established to construct the fire prediction model. Both MODIS and GOES fire observations show that the NWP-based fire prediction model is an improvement over the forecast of persistence commonly used by near-real-time fire emission inventories. Results from an independent test (2005 fire season) show that the root-mean-square error (RMSE) of predicted MODIS fire observations is reduced by 5.2% compared with a persistence forecast. Improvements are strongest (RMSE reduction of 11.4%) for cases with observed decay or extinction of fires. Similar results are obtained from additional independent tests using the 2004 and 2005 GOES satellite fire observations. This study uniquely demonstrates the value and importance of combining NWP data and satellite fire observations to predict biomass-burning emissions, which is a critical step toward producing a global short-term fire prediction model and improving operational forecasts of smoke transport at large spatial scales.

1. Introduction

Smoke produced by global biomass burning is a key source of aerosol particles, greenhouse gases, and other trace constituents in the atmosphere, which affect the global climate system by altering atmospheric composition and radiative processes (e.g. Randerson et al., 2006; Spracklen et al., 2007; Jordan et al., 2008; Kopacz et al., 2011). The combination of an intense fire event with

* Corresponding author. Present address: Naval Research Laboratory in Monterey, CA, USA. Tel.: +1 831 656 4093.
E-mail addresses: david.peterson.ctr@nrlmry.navy.mil (D. Peterson), edward.hyer@nrlmry.navy.mil (E. Hyer), jwang7@unl.edu (J. Wang).

1352-2310/$ – see front matter © 2013 Elsevier Ltd. All rights reserved.
http://dx.doi.org/10.1016/j.atmosenv.2013.01.052

suitable atmospheric conditions (Kahn et al., 2007, 2008; Val Martin et al., 2010) can allow smoke particles to be injected above the boundary layer, and transported thousands of miles (e.g. Westphal and Toon, 1991; Damoah et al., 2006; Sapkota et al., 2005; Duck et al., 2007). These intense fire events, common in the boreal forest of North America, affect air quality and visibility, create health concerns, and may interact with meteorological processes at a great distance from a fire (e.g. Wang and Christopher, 2006; Wang et al., 2006, 2013). Several global and regional inventories of biomass burning emissions have been developed over the past decade in an effort to quantify sources and transport of aerosol particles and trace gases. Examples include the Fire Locating and Monitoring of Burning Emissions (FLAMBÉ), produced by the Naval Research Laboratory (Reid et al., 2009), the Fire Inventory from NCAR (FINN), produced by the National Center for Atmospheric Research (Wiedinmyer et al., 2011), the Global Fire Emissions Database (GFED) (van der Werf et al., 2010; Mu et al., 2011), the Global Fire Assimilation System (GFAS) (Kaiser et al., 2011), and the emissions inventory produced by the National Oceanic and Atmospheric Administration (Zhang et al., 2008, 2012). While the methodology of these emissions inventories varies, the first step for systems operating in near real time is always dependent on observations of active fires, because they are the only consistent source of data over continental scales available in near real time. The observed spatial and temporal patterns of satellite fire observations drive the patterns of estimated smoke emissions from these systems.

Across the globe, biomass-burning activity is highly sensitive to the local climate, including variations in the synoptic weather pattern (e.g. Brotak and Reifsnyder, 1977). In the boreal forest, the fire season is short relative to other ecosystems, and a large majority of fire activity is often concentrated in just a few days of active burning (Hyer et al., 2007). Active fire seasons have been linked to positive 500 hPa geopotential height anomalies (Skinner et al., 1999, 2002), which must persist for approximately 10 days (Fauria and Johnson, 2006). This synoptic environment is conducive to active fire weather conditions at the surface, such as warmer temperatures and suppressed precipitation. The duration of dry conditions typically has a much stronger relation to burned area observations than the total seasonal precipitation (e.g. Flannigan and Harrington, 1988), and therefore sets the stage for active fire weather conditions (Peterson et al., 2010). In addition, low-level instability has been linked to intense fire activity (e.g. Haines, 1988; Potter et al., 2008), and may increase the potential for fire ignition via dry lightning strikes, provided the synoptic environment is favorable (Peterson et al., 2010). Unstable conditions may also result in higher smoke plumes, stronger entrainment of the air near the fires, and faster spread rate, all of which can lead to "extreme fire behavior" and pyroconvection (e.g. Werth and Ochoa, 1993; Fromm et al., 2010).

While the synoptic environment is a useful first step, additional information is required to characterize variations in localized, short-term meteorological conditions and their effect on fire observations, especially when managing active fires that may threaten life and property. As a result, over 30 years of research has focused the development of several fire weather indices that are currently used operationally in boreal North America. The most well-known of these, the Canadian Forest Fire Danger Rating System (CFFDRS), uses surface temperature, relative humidity, rainfall, and wind speed to derive the biomass moisture content used for assessing daily fire potential and spread in the unique boreal ecosystem (Van Wagner and Pickett, 1985; Van Wagner, 1987; Amiro et al., 2004). The CFFDRS is typically calculated using observations from nearby weather stations, however large regions within the boreal forest are sparsely populated, limiting the available observations. Therefore, a continuous source of weather data via Numerical Weather Prediction (NWP) is highly desirable, especially when trying to develop an automated fire weather forecast in the boreal regions. Mölders (2008) showed that the Weather Research and Forecasting (WRF) model, at a fairly coarse spatiotemporal resolution of 1.0° and 6-h, can successfully calculate fire weather indices in interior Alaska, assuming the corresponding meteorological variables are accurately predicted. Therefore, the current study explores the potential for using NWP data to capture day-to-day changes in fire activity.

This study is further motivated by the fact that all near-real-time fire emission inventories, including FLAMBÉ, which is used operationally by the Navy Aerosol Analysis and Prediction System (NAAPS) at the Fleet Numerical Meteorological and Oceanographic Center (the US Navy's forecast center), use observations of fire pixels (known as fire counts) from geostationary and polar-orbiting satellite sensors (e.g. Reid et al., 2009). For numerical forecasting of smoke, however, FLAMBÉ and other models typically assume that the number of observed fire counts does not change throughout the forecast period – a forecast of persistence. This may result in large errors in the final smoke emissions forecast, especially due to changes in local meteorological conditions, which undoubtedly affect fire activity. Therefore, drawing from continued improvements in NWP accuracy, the current study makes the first attempt at developing an automated, NWP-based statistical model that can be used to characterize the effect of a given set of meteorological conditions on the following day's satellite-observed fire counts, including ignition and spread potential, with the ultimate goal of enhancing the estimation and forecast of smoke emissions at large spatial scales.

2. Study region and data

Drawing from a copious base of previous research and the potential for very large, intense fire events, the North American boreal forest is an ideal location for developing a fire count prediction model. The specific study region, located primarily in Alaska, is based on Peterson et al. (2010) and includes the core of the mountainous western boreal forest (Fig. 1a). Within the study region, the fire season typically falls between May and September (Skinner et al., 1999; Stocks et al., 2002; Fauria and Johnson, 2006), and the fire seasons of 2004 and 2005 were two of the three largest in the 73-year observational record (Kasischke et al., 2002). The MODIS sensors aboard the Terra (launched in 1999) and Aqua (launched in 2002) satellites are the primary source of fire count data (MOD14) in this study (Giglio et al., 2003; Giglio, 2010), and the GOES Wildfire Automated Biomass Burning Algorithm (WF_ABBA) fire product (Prins and Menzel, 1994; Prins et al., 1998) is used for independent testing of the algorithm.

As a polar-orbiting sensor, the MODIS fire detections are not a perfect indicator of fire activity, and have known biases including the inability to detect fires beneath opaque clouds and large variations in pixel size depending on the satellite viewing zenith angle (Masuoka et al., 1998; Gomez-Landesa et al., 2004). However, MODIS data are best suited for developing a fire prediction model for the study region because: (a) MODIS observed fire counts are a primary source for estimates of fire emissions in FLAMBÉ and FINN, (b) MODIS has the ability to detect smaller fires relative to GOES, and (c) MODIS may be better suited for high-latitude locations than GOES.

For the meteorological component of this study, data are obtained from the North American Regional Reanalysis (NARR), which blends a variety of observational data into Eta model output containing 45 vertical layers across the North American continent with ~32 km grid spacing every 3 h (Ebisuzaki, 2004; Mesinger et al., 2006). The NARR data are also used to produce three modified components of the CFFDRS that are relevant to short-term changes

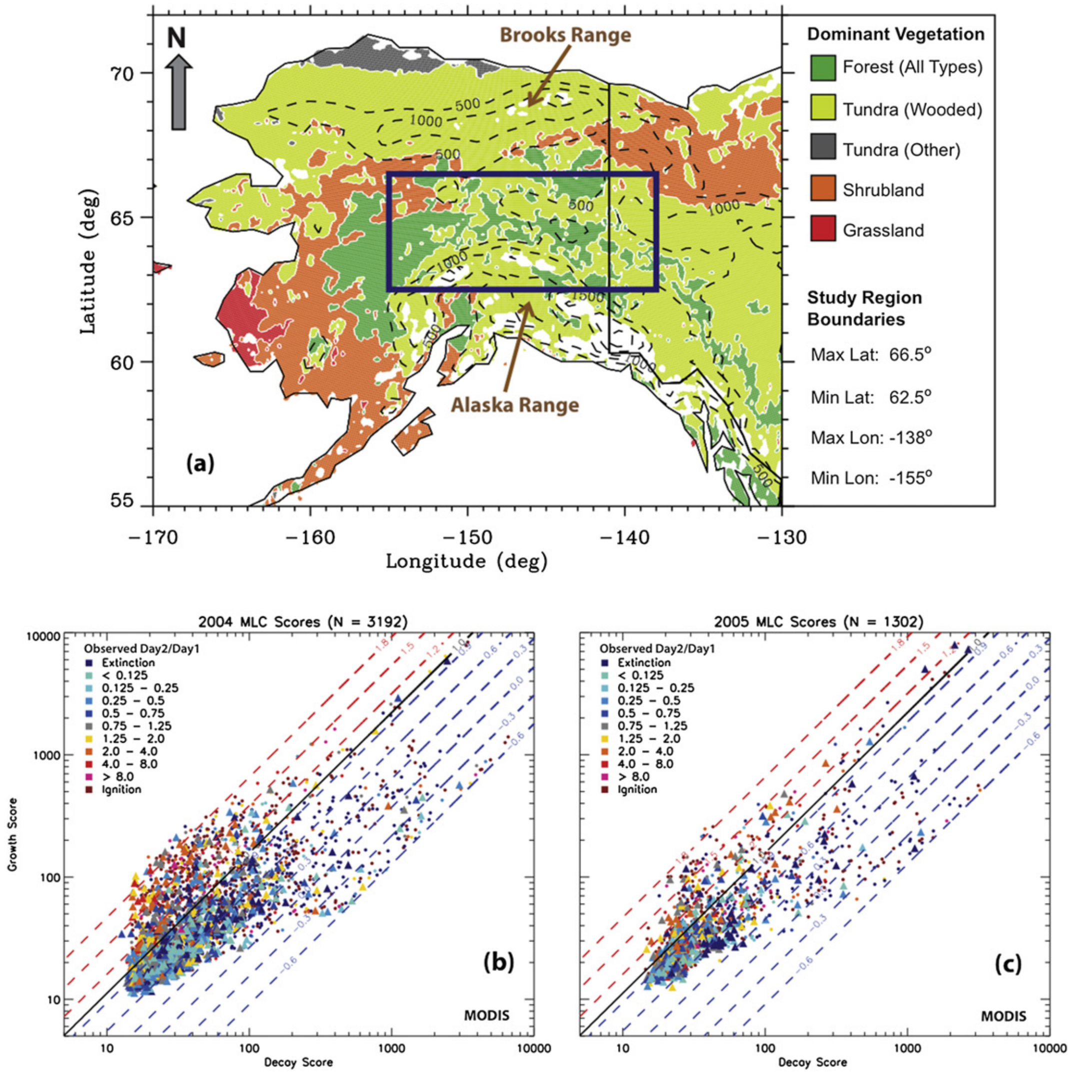

Fig. 1. (a) Map highlighting the boreal study region as a blue box. The color scheme is based on the dominant vegetation types located within and surrounding the study region. Dashed black contours indicate variations in topography, with a contour interval of 500 m. (b) and (c) Output of MLC_{grow} and MLC_{decay} from the 2004 development test and the 2005 independent test, respectively. Small circles indicate where the number of MODIS fire counts on day 1 are <10 and large triangles indicate where the day 1 fire counts are at least 10. The color scheme indicates the observed relative change in fire counts (or ΔFC_{obs}). Red and blue contours indicate the prediction score (or ΔFC_p) obtained from a multiple regression as a function of MLC_{grow} and MLC_{decay}. The black contour indicates no change or a forecast of persistence ($\Delta FC_p = 1$).

in fire activity, including (1) the fine fuel moisture code (FFMC) describing the moisture content of the fine plant litter in a thin layer on the forest floor, (2) the initial spread index (ISI) created from the combination of the FFMC and surface wind speed, and (3) the fire weather index (FWI), which is created from all six CFFDRS components and describes the overall fire weather situation for the next 24 h (Van Wagner and Pickett, 1985; Van Wagner, 1987). Drawing from the fire weather relationships identified by Peterson et al. (2010), additional indices are also computed to describe the ignition potential, synoptic influence, and the moisture deficit affecting boreal wildfire activity. Therefore, a large suite of meteorological information, including both single variables and fire weather indices for day 1 (observation) and day 2 (forecast), are available to this study. To facilitate the analysis, the MODIS (or GOES) fire counts are geographically matched onto the mesh of NARR grid boxes. All fire counts observations are then summed over each individual NARR grid box per day, based on the temporal requirements of the CFFDRS (18:00Z to 18:00Z). The CFFDRS are calculated at 10 AM local time (18:00Z) rather than at noon (operational standard) in an effort to define a single observation time that can be used across the boreal forest of North America and to match the daytime MODIS observations (~10:30 AM and 1:30 PM local time), which typically contain the maximum daily fire activity (Ichoku et al., 2008).

3. Statistical prediction of fire growth and decay

The primary goal of the prediction model is to establish an empirical relationship between weather, fire ignition, and fire evolution, expressed in terms of the change in MODIS fire counts (day 1 vs. day 2) as a function of meteorological variables and fire weather indices. The specific methodology is largely based on a Maximum Likelihood Classification (MLC) score, which is given by

$$MLC_i(x) = -\ln\left|\sum_i\right| - (x_{input} - m_i)^t \sum_i^{-1} (x_{input} - m_i) \qquad (1)$$

where m_i and Σ_i are the mean vector and covariance matrix for a predetermined number (i) of training classes (Richards and Jia, 2006). This method is widely used in satellite remote sensing for the classification of images (into vegetation, water, clouds, etc.), where m_i and Σ_i are computed from training data (a pre-selected vector of radiometric data x_{training} at various spectral channels) corresponding to each class i. For any given vector of input data (x_{input}), its MLC score, or the likelihood for x_{input} to be in class i, is computed via Equation (1), and x_{input} is assigned to the class that provides the largest MLC score.

In an analogy to image classification, the MLC technique can be applied to classify the day-to-day change in fire counts based on a variety of meteorological factors that form the elements of the vector x_{input} in Equation (1). To begin, the change in observed MODIS fire counts between day 1 and day 2 are stratified into five classes for each ~32 km grid cell of the NARR: (1) ignition, (2) extinction, (3) growth, (4) decay, and (5) no change. Limitations in satellite fire data (e.g. cloud cover and scan-to-scan variations) can create false ignition and extinction events, so the current version of the MLC is largely based on classes (3) and (4). The primary goal is to capture large changes in the number of fire counts (either growth or decay per grid box) because these are the cases where the total smoke emissions are likely to change significantly. Therefore, training data are defined from the largest cases, defined by the 75th percentile, within the growth and decay fire count classes, from which m_i and Σ_i are computed. Finally, the x_{input} corresponding to each individual event is compared to m_i and Σ_i via Equation (1), thus producing the MLC growth (MLC_{grow}) and decay ($\text{MLC}_{\text{decay}}$) scores. The complete list of inputs used to create x_{input} is provided in Table 1, and includes the fire weather indices and other single variables, such as relative humidity and convective available potential energy (CAPE), that display the largest separability between cases of fire growth and decay. Therefore, the modified MLC output determines whether a given fire event best fits the growth or decay fire class.

While the MLC training data are only derived from fire classes (3) and (4), the MLC_{grow} and $\text{MLC}_{\text{decay}}$ scores can be computed for all five classes. Fig. 1b shows an example MLC output for the large 2004 fire season, with 3192 NARR grid boxes containing fire pixels in central Alaska. The output is provided in a log scale, and cases of observed growth and decay are evidently concentrated in distinct clusters. However, it is also evident that many NARR grid boxes, especially those with <10 MODIS fire counts on day 1 (small circles in Fig. 1b), are misclassified, which likely results from the uncertainty introduced by scan-to-scan variations of the MODIS sensor. Therefore, emphasis is placed on grid boxes with at least 10 fire counts on day 1 (large triangles in Fig. 1b), ensuring the fire is large in size and likely to appear in a subsequent scan.

Table 1
Input variables for the MLC.

Input variable	
Ratios (Day 2/Day 1)	
1	Fire Weather Index (FWI)
2	Initial Spread Index (ISI)
3	Fine Fuel Moisture Content (FFMC)
4	Synoptic Index (500 hPa Heights, ISI, & Dry Days)[a]
5	Moisture Index (Consecutive Dry Days & FFMC)[a]
6	Relative Humidity
Daily variables	
7	Day 1 Initial Spread Index (ISI)
8	Day 1 Fine Fuel Moisture Content (FFMC)
9	Day 1 Ignition Index (CAPE & 500 hPa Heights)[a]
10	Day 1 Moisture Index (Consecutive Dry Days & FFMC)[a]
11	Day 1 Conv. Available Pot. Energy (CAPE)
12	Day 2 Conv. Available Pot. Energy (CAPE)
Other	
13	Observed Fire Count Tendency (Previous 3 Days)

[a] Additional fire weather indices developed specifically for this study.

The MLC_{grow} and $\text{MLC}_{\text{decay}}$ scores for the large symbols in Fig. 1b indicate that the training data, which are drawn from limited data samples (e.g. 75th percentile), generally capture the statistics that needed to separate the growth and decay of the fires. In a real atmosphere, meteorological variables generally co-vary, and therefore the observed relative change in fire counts ($\Delta\text{FC}_{\text{obs}}$) will relate to both the magnitude and relative values of MLC_{grow} and $\text{MLC}_{\text{decay}}$: a larger growth score and small decay score may indicate larger $\Delta\text{FC}_{\text{obs}}$. As a result, the MLC output is further refined via a linear regression of MLC_{grow} and $\text{MLC}_{\text{decay}}$ against $\Delta\text{FC}_{\text{obs}}$ to produce a fire count prediction score (ΔFC_p)

$$\Delta\text{FC}_p = a_1\ln(\text{MLC}_{\text{grow}}) + a_2\ln\left(\text{MLC}_{\text{decay}}\right) + a_0 \tag{2}$$

where a_1 and a_2 respectively equal the slopes for growth and decay (calculated from only the large day 1 cases, triangles in Fig. 1b) and a_0 is a constant. The resulting contour lines of ΔFC_p for all data points are also overlaid on Fig. 1b, c (blue and red parallel lines).

As described above, Equations (1) and (2) are the two key steps in the fire prediction methodology for the meteorological input vector (x_{input}). First, MLC_{grow} and $\text{MLC}_{\text{decay}}$ are computed using Equation (1), and the regression Equation (2) is subsequently used to compute ΔFC_p. As shown in Fig. 2a, this ΔFC_p score can then be evaluated against the true $\Delta\text{FC}_{\text{obs}}$ (here the absolute change in fire counts) for all the cases in 2004. It is found that while the ΔFC_p score and $\Delta\text{FC}_{\text{obs}}$ are consistent in terms of sign, there are considerable deviations from the 1:1 line. In order to transform ΔFC_p into a quantitative predictor, the extinction and ignition cases are removed, as well as cases with small day 1 fire counts, and a running mean and median are applied to the remaining cases (blue curves in Fig. 2b). Based on the running mean and median curves, four parameters are empirically estimated to derive the three-zone quantitative predictor (displayed as a brown curve in Fig. 2b): (1) the slope of the growth zone (M_{grow}), which relates $\Delta\text{FC}_{\text{obs}}$ to the predicted growth in fire counts, (2) the slope of the decay zone (M_{decay}), which relates $\Delta\text{FC}_{\text{obs}}$ to the predicted decay in fire counts, (3–4) the lower and upper bounds of the persistence zone ($P_{\min}$ and $P_{\max}$), where no change will be forecast. When ΔFC_p is above $P_{\max}$, growth is forecast as $(\Delta\text{FC}_p - P_{\max})^*M_{\text{grow}}$, and when ΔFC_p is below $P_{\min}$, decay is forecast as $(\Delta\text{FC}_p - P_{\min})^*M_{\text{decay}}$. This quantitative predictor is analogous to a step commonly used in the Model Output Statistics (MOS) for a weather forecast, where NWP output, (here the regression model) is further corrected/adjusted to produce a final forecast (Wilks, 2006). Parameters (1–4) are derived using only the 2004 MODIS fire counts, and subsequently applied to all tests using MODIS and GOES fire count data for 2004 and 2005.

4. Evaluating the fire count prediction model

When applying the fire count prediction model to all available data, including ignition and extinction cases, the results from the 2004 MODIS test (used to develop the model) suggest the RMSE can be reduced by 13.1% compared to a forecast of persistence – the method currently employed in FLAMBÉ and other operational emission products (Table 2). A larger reduction in error is obtained for cases where decay or extinction occurred (reduction in RMSE = 24.3%), partly because decay/extinction processes are often abrupt, driven by precipitation. When comparing these results to an independent test, conducted by applying the prediction model to the fire season of 2005, a smaller but still significant 11.4% reduction in RMSE is observed for cases where decay/extinction occurred, as well as an overall reduction in RMSE. However, the growth/ignition predictions do not seem to offer an improvement over a forecast of persistence. The reason for this is clear from the 2005 MLC scores,

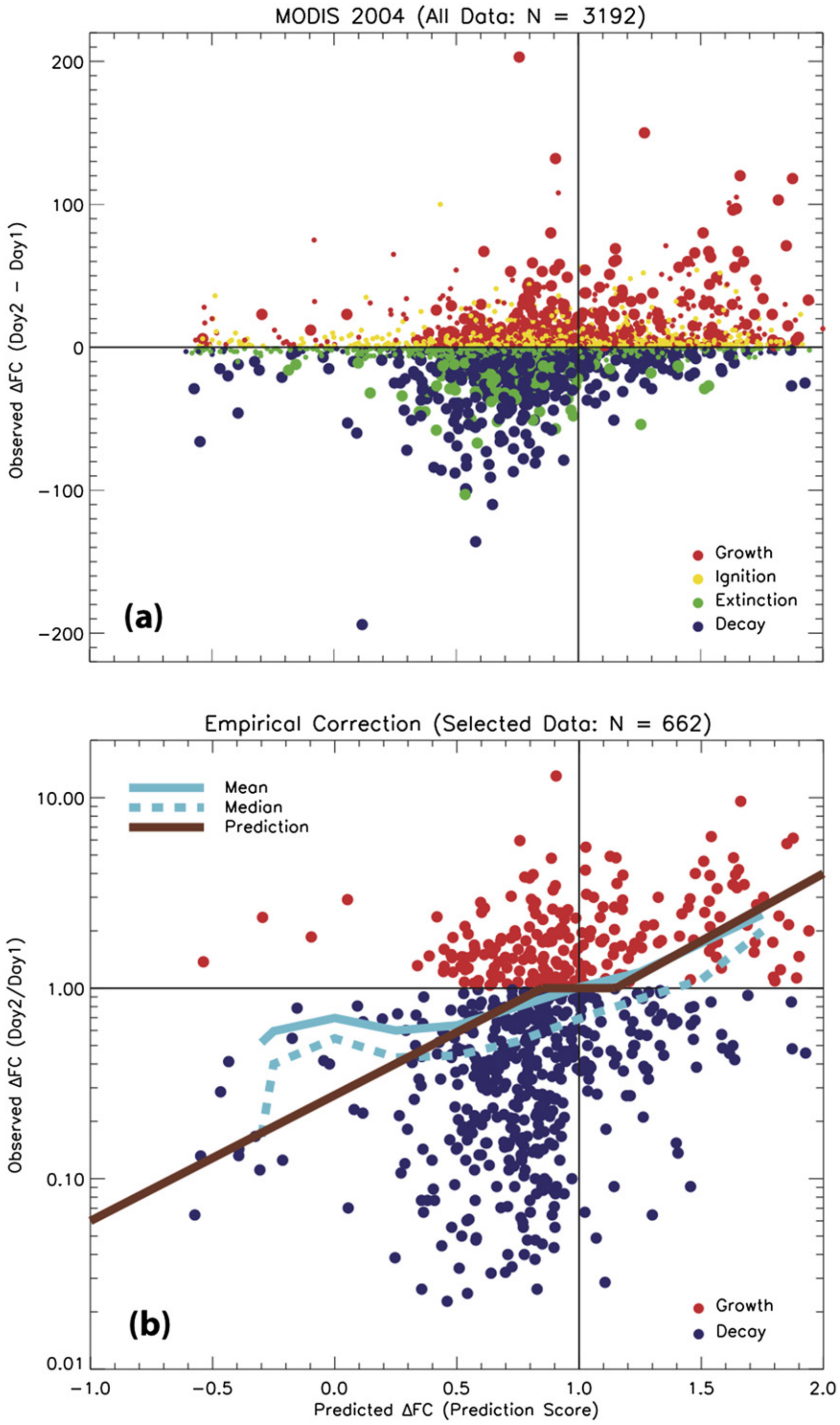

Fig. 2. Results of the multiple regression function displayed as red and blue contours in Fig. 1b. (a) Comparison between the prediction score (ΔFC_p) and the observed absolute change in fire counts (day 2 − day 1, ΔFC_{obs}) for all data points. Small symbols indicate where the number of fire counts on day 1 are <10 and large symbols indicate where the day 1 fire counts are at least 10. (b) Comparison between the prediction score (ΔFC_p) and the observed relative change in fire counts (day 2/day 1, ΔFC_{obs}) with the ignition, extinction, and small day 1 cases (small symbols) removed. The brown line indicates the three-zone quantitative predictor curve that is based on the running mean and median, which are respectively displayed as solid and dashed blue curves.

displayed in Fig. 1c, where decay/extinction cases are found in a distinct cluster while many growth/ignition cases are misclassified.

While the fire count prediction methodology was developed using MODIS, the same MLC output (m_i and Σ_i in Equation (1)) can also be applied to GOES observations, or any other satellite sensor. The resulting independent tests for GOES (Table 2) yield similar results to MODIS, with an overall reduction in RMSE for both 2004 and 2005, due in part to large RMSE reductions in cases of decay/extinction. The agreement between the MODIS and GOES tests shows that the fire count prediction is a robust fire count prediction for the western boreal forest of North America. In addition, Table 2 shows that experimenting with various combinations of the day 1 and day 2 components of the CFFDRS alone (e.g. FWI, ISI, and FFMC) does not produce better results than the larger combination of

Table 2
RMSE statistics for the fire count prediction model compared to persistence.

Observation	N	Persistence	CFFDRS inputs only		All inputs (Table 1)	
		RMSE	RMSE	% change	RMSE	% change
2004 Development test (MODIS)						
Overall	3192	18.3	17.6	**−4.1**	15.9	**−13.1**
Growth/Ignition	435	34.6	34.5	**−0.1**	32.9	**−5.0**
Persistence[a]	2328	4.0	4.2	5.6	4.4	11.2
Decay/Extinction	429	34.6	31.4	**−9.1**	26.2	**−24.3**
2005 Independent test (MODIS)						
Overall	1302	21.2	20.6	**−3.1**	20.1	**−5.2**
Growth/Ignition	228	33.5	34.0	1.5	34.0	1.5
Persistence[a]	857	4.1	4.2	1.5	4.1	0.5
Decay/Extinction	217	38.1	35.4	**−7.2**	33.8	**−11.4**
2004 Independent test (GOES)						
Overall	1235	7.6	7.4	**−1.7**	7.1	**−6.1**
Growth/Ignition	236	11.2	11.4	1.2	11.4	1.2
Persistence[a]	768	2.2	2.2	**−1.4**	2.2	**−1.4**
Decay/Extinction	231	12.7	12.1	**−4.2**	11.0	**−13.0**
2005 Independent test (GOES)						
Overall	821	7.6	7.6	**−0.7**	7.3	**−4.1**
Growth/Ignition	177	11.0	11.1	1.2	11.1	1.00
Persistence[a]	485	2.2	2.3	2.7	2.2	**−0.5**
Decay/Extinction	159	12.3	12.0	**−2.7**	11.1	**−9.3**

Bold font indicates a reduction in RMSE.
[a] Observed persistence is bounded by ±10 and ±5 fire counts for MODIS and GOES, respectively.

variables displayed in Table 1, suggesting that the additional considerations of low-level instability (e.g. CAPE), ignition potential, and general synoptic conditions are necessary for x_{input} and the resulting fire count prediction.

5. Discussion and conclusions

This study has taken the first step toward linking day-to-day changes in satellite fire counts to variations in meteorological variables obtained from NWP using an MLC-based prediction model in the North American boreal forest. While MODIS fire counts are affected by the daily variation of several unavoidable factors, including the location within the scan (viewing angle) and cloud cover, the 2005 independent tests (for both MODIS and GOES) indicate that the decay/extinction prediction alone can be incorporated as an improvement over persistence, thus yielding a forecast of either persistence or decay/extinction. The results also show that the current suite of fire weather indices (e.g. the CFFDRS) must be supplemented with additional variables (e.g. CAPE) to improve prediction accuracy at the daily regional scale.

As shown in this study, forecasting the decay of a fire event is often a simpler problem compared with fire growth, primarily due to the impact from precipitation events. However, several meteorological variables that greatly impact fire ignition and growth, such as lightning strikes, are either unreliable or unavailable in the current NWP output. Therefore, the prediction methodology must be further refined to improve growth/ignition predictions, perhaps by accounting for holdover effects from previous lightning strikes or incorporating additional satellite fire products. In the near future, higher resolution (and spatially uniform) fire data from NPP VIIRS (Csiszar et al., 2011) and improved lightning data from GOES-R (http://www.goes-r.gov), can be used in combination with a modified measure of fire radiative power, scaled by the retrieved, instantaneous fire area (Peterson et al., 2013; Peterson and Wang, 2013), as additional inputs for the fire prediction model. These potential improvements warrant future studies in an effort to achieve the ultimate goal of producing a global fire prediction model (with similar NWP input variables) that can be ingested into the smoke emissions modeling process (e.g. FLAMBÉ), allowing a 24-h or longer forecast of smoke emissions to be calculated based on the predicted change in fire activity.

Acknowledgments

This project was funded by the Naval Research Enterprise Intern Program (summer 2011) at the Naval Research Laboratory in Monterey, California and by the NASA Earth and Space Science Fellowship (to D. Peterson). We are also grateful to the support from NASA's Suomi-NPP Program, Applied Science Program, and Radiation Sciences Program.

References

Amiro, B.D., Logan, K.A., Wotton, B.M., Flannigan, M.D., Todd, J.B., Stocks, B.J., Martell, D.L., 2004. Fire weather index system components for large fires in the Canadian boreal forest. International Journal of Wildland Fire 13, 391–400.
Brotak, E.A., Reifsnyder, W.E., 1977. Investigation of synoptic situations associated with major wildland fires. Journal of Applied Meteorology 16, 867–870.
Csiszar, I.A., Schroeder, W., Giglio, L., Justice, C.O., Ellicott, E., 2011. Quantitative Evaluation of Active Fire Detection Capabilities from VIIRS. 91st American Meteorological Society Annual Meeting, Seattle, WA.
Damoah, R., Spichtinger, N., Servranckx, R., Fromm, M., Eloranta, E.W., Razenkov, I.A., James, P., Shulski, M., Forster, C., Stohl, A., 2006. A case study of pyro-convection using transport model and remote sensing data. Atmospheric Chemistry and Physics 6, 173–185.
Duck, T.J., Firanski, B.J., Millet, D.B., Goldstein, A.H., Allan, J., Holzinger, R., Worsnop, D.R., White, A.B., Stohl, A., Dickinson, C.S., van Donkelaar, A., 2007. Transport of forest fire emissions from Alaska and the Yukon Territory to Nova Scotia during summer 2004. Journal of Geophysical Research: Atmospheres 112.
Ebisuzaki, W., 2004. In: NOAA (Ed.), National Climatic Data Center Data Documentation for NOAA Operational Model Archive and Distribution System (NOMADS) North American Regional Reanalysis, pp. 1–11. Camp Springs, MD.
Fauria, M.M., Johnson, E.A., 2006. Large-scale climatic patterns control large lightning fire occurrence in Canada and Alaska forest regions. Journal of Geophysical Research: Biogeosciences 111.
Flannigan, M.D., Harrington, J.B., 1988. A study of the relation of meteorological variables to monthly provincial area burned by wildfire in Canada (1953–80). Journal of Applied Meteorology 27, 441–452.
Fromm, M., Lindsey, D.T., Servranckx, R., Yue, G., Trickl, T., Sica, R., Doucet, P., Godin-Beekmann, S.E., 2010. The untold story of pyrocumulonimbus. Bulletin of the American Meteorological Society 91, 1193–1209.
Giglio, L., 2010. MODIS Collection 5 Active Fire Product User's Guide Version 2.4. University of Maryland, Department of Geography, pp. 1–61.
Giglio, L., Descloitres, J., Justice, C.O., Kaufman, Y.J., 2003. An enhanced contextual fire detection algorithm for MODIS. Remote Sensing of Environment 87, 273–282.
Gomez-Landesa, E., Rango, A., Bleiweiss, M., 2004. An algorithm to address the MODIS bowtie effect. Canadian Journal of Remote Sensing 30, 644–650.
Haines, D.A., 1988. A Lower Atmosphere Severity Index for Wildland Fire. National Weather Digest, pp. 23–27.
Hyer, E.J., Kasischke, E.S., Allen, D.J., 2007. Effects of source temporal resolution on transport simulations of boreal fire emissions. Journal of Geophysical Research: Atmospheres 112.
Ichoku, C., Giglio, L., Wooster, M.J., Remer, L.A., 2008. Global characterization of biomass-burning patterns using satellite measurements of fire radiative energy. Remote Sensing of Environment 112, 2950–2962.
Jordan, N.S., Ichoku, C., Hoff, R.M., 2008. Estimating smoke emissions over the US Southern Great Plains using MODIS fire radiative power and aerosol observations. Atmospheric Environment 42, 2007–2022.
Kahn, R.A., Chen, Y., Nelson, D.L., Leung, F.-Y., Li, Q., Diner, D.J., Logan, J.A., 2008. Wildfire smoke injection heights: two perspectives from space. Geophysical Research Letters 35.
Kahn, R.A., Li, W.H., Moroney, C., Diner, D.J., Martonchik, J.V., Fishbein, E., 2007. Aerosol source plume physical characteristics from space-based multiangle imaging. Journal of Geophysical Research: Atmospheres 112, 20.
Kaiser, J.W., Heil, A., Andreae, M.O., Benedetti, A., Chubarova, N., Jones, L., Morcrette, J.J., Razinger, M., Schultz, M.G., Suttie, M., van der Werf, G.R., 2011. Biomass burning emissions estimated with a global fire assimilation system based on observed fire radiative power. Biogeosciences 9, 527–554.
Kasischke, E.S., Williams, D., Barry, D., 2002. Analysis of the patterns of large fires in the boreal forest region of Alaska. International Journal of Wildland Fire 11, 131–144.
Kopacz, M., Mauzerall, D.L., Wang, J., Leibensperger, E.M., Henze, D.K., Singh, K., 2011. Origin and radiative forcing of black carbon transported to the Himalayas and Tibetan Plateau. Atmospheric Chemistry and Physics 11, 2837–2852.

Masuoka, E., Fleig, A., Wolfe, R.E., Patt, F., 1998. Key characteristics of MODIS data products. IEEE Transactions on Geoscience and Remote Sensing 36, 1313–1323.
Mesinger, F., DiMego, G., Kalnay, E., Mitchell, K., Shafran, P.C., Ebisuzaki, W., Jovi, Du, Woollen, J., Rogers, E., Berbery, E.H., Ek, M.B., Fan, Y., Grumbine, R., Higgins, W., Li, H., Lin, Y., Manikin, G., Parrish, D., Shi, W., 2006. North American regional reanalysis. Bulletin of the American Meteorological Society 87, 343–360.
Mölders, N., 2008. Suitability of the weather research and forecasting (WRF) model to predict the June 2005 fire weather for interior Alaska. Weather and Forecasting 23, 953–973.
Mu, M., Randerson, J.T., van der Werf, G.R., Giglio, L., Kasibhatla, P., Morton, D., Collatz, G.J., DeFries, R.S., Hyer, E.J., Prins, E.M., Griffith, D.W.T., Wunch, D., Toon, G.C., Sherlock, V., Wennberg, P.O., 2011. Daily and 3-hourly variability in global fire emissions and consequences for atmospheric model predictions of carbon monoxide. Journal of Geophysical Research: Atmospheres 116.
Peterson, D., Wang, J., Ichoku, C., Remer, L.A., 2010. Effects of lightning and other meteorological factors on fire activity in the North American boreal forest: implications for fire weather forecasting. Atmospheric Chemistry and Physics 10, 6873–6888.
Peterson, D., Wang, J., 2013. A sub-pixel-based calculation of fire radiative power from MODIS observations: 2. Sensitivity analysis and potential fire weather application. Remote Sensing of Environment 129, 231–249.
Peterson, D., Wang, J., Ichoku, C., Hyer, E., Ambrosia, V., 2013. A sub-pixel-based calculation of fire radiative power from MODIS observations: 1. Algorithm Development and Initial Assessment. Remote Sensing of Environment 129, 262–279.
Potter, B.E., Winkler, J.A., Wilhelm, D.F., Shadbolt, R.P., 2008. Computing the low-elevation variant of the Haines index for fire weather forecasts. Weather and Forecasting 23, 159–167.
Prins, E.M., Feltz, J.M., Menzel, W.P., Ward, D.E., 1998. An overview of GOES-8 diurnal fire and smoke results for SCAR-B and 1995 fire season in South America. Journal of Geophysical Research: Atmospheres 103, 31821–31835.
Prins, E.M., Menzel, W.P., 1994. Trends in South-American biomass burning detected with the GOES visible infrared spin scan radiometer atmospheric sounder from 1983 to 1991. Journal of Geophysical Research: Atmospheres 99, 16719–16735.
Randerson, J.T., Liu, H., Flanner, M.G., Chambers, S.D., Jin, Y., Hess, P.G., Pfister, G., Mack, M.C., Treseder, K.K., Welp, L.R., Chapin, F.S., Harden, J.W., Goulden, M.L., Lyons, E., Neff, J.C., Schuur, E.A.G., Zender, C.S., 2006. The impact of boreal forest fire on climate warming. Science 314, 1130–1132.
Reid, J.S., Hyer, E.J., Prins, E.M., Westphal, D.L., Zhang, J.L., Wang, J., Christopher, S.A., Curtis, C.A., Schmidt, C.C., Eleuterio, D.P., Richardson, K.A., Hoffman, J.P., 2009. Global monitoring and forecasting of biomass-burning smoke: description of and lessons from the Fire Locating and Modeling of Burning Emissions (FLAMBE) program. IEEE Journal of Selected Topics in Applied Earth Observations and Remote Sensing 2, 144–162.
Richards, J.A., Jia, X., 2006. Supervised Classification Techniques, Remote Sensing Digital Image Analysis: an Introduction, fourth ed. Springer-Verlag, Berlin Heidelberg, pp. 192–204.
Sapkota, A., Symons, J.M., Kleissl, J., Wang, L., Parlange, M.B., Ondov, J., Breysse, P.N., Diette, G.B., Eggleston, P.A., Buckley, T.J., 2005. Impact of the 2002 Canadian forest fires on particulate matter air quality in Baltimore City. Environmental Science & Technology 39, 24–32.
Skinner, W.R., Flannigan, M.D., Stocks, B.J., Martell, D.L., Wotton, B.M., Todd, J.B., Mason, J.A., Logan, K.A., Bosch, E.M., 2002. A 500 hPa synoptic wildland fire climatology for large Canadian forest fires, 1959–1996. Theoretical and Applied Climatology 71, 157–169.
Skinner, W.R., Stocks, B.J., Martell, D.L., Bonsal, B., Shabbar, A., 1999. The association between circulation anomalies in the mid-troposphere and area burned by wildland fire in Canada. Theoretical and Applied Climatology 63, 89–105.
Spracklen, D.V., Logan, J.A., Mickley, L.J., Park, R.J., Yevich, R., Westerling, A.L., Jaffe, D.A., 2007. Wildfires drive interannual variability of organic carbon aerosol in the western US in summer. Geophysical Research Letters 34.
Stocks, B.J., Mason, J.A., Todd, J.B., Bosch, E.M., Wotton, B.M., Amiro, B.D., Flannigan, M.D., Hirsch, K.G., Logan, K.A., Martell, D.L., Skinner, W.R., 2002. Large forest fires in Canada, 1959–1997. Journal of Geophysical Research: Atmospheres 108.
Val Martin, M., Logan, J.A., Kahn, R.A., Leung, F.Y., Nelson, D.L., Diner, D.J., 2010. Smoke injection heights from fires in North America: analysis of 5 years of satellite observations. Atmospheric Chemistry and Physics 10, 1491–1510.
van der Werf, G.R., Randerson, J.T., Giglio, L., Collatz, G.J., Mu, M., Kasibhatla, P.S., Morton, D.C., DeFries, R.S., Jin, Y., van Leeuwen, T.T., 2010. Global fire emissions and the contribution of deforestation, savanna, forest, agricultural, and peat fires (1997–2009). Atmospheric Chemistry and Physics 10, 11707–11735.
Van Wagner, C.E., Pickett, T.L., 1985. In: Service, C.F. (Ed.), Equations and FORTRAN Program for the Canadian Forest Fire Weather Index System. Government of Canada, Ottawa.
Van Wagner, C.E., 1987. Development and Structure of the Canadian Forest Fire Weather Index System. Canadian Forestry Service.
Wang, J., Ge, C., Yang, Z., Hyer, E.J., Reid, J.S., Chew, B.N., Mahmud, M., Zhang, Y., Zhang, M., 2013. Mesoscale modeling of smoke transport over the Southeast Asian Maritime Continent: interplay of sea breeze, trade wind, typhoon, and topography. Atmospheric Research 122, 486–503.
Wang, J., Christopher, S.A., 2006. Mesoscale modeling of Central American smoke transport to the United States: 2. Smoke radiative impact on regional surface energy budget and boundary layer evolution. Journal of Geophysical Research: Atmospheres 111.
Wang, J., Christopher, S.A., Nair, U.S., Reid, J.S., Prins, E.M., Szykman, J., Hand, J.L., 2006. Mesoscale modeling of Central American smoke transport to the United States: 1. "Top-down" assessment of emission strength and diurnal variation impacts. Journal of Geophysical Research: Atmospheres 111.
Werth, P., Ochoa, R., 1993. The evaluation of Idaho wildfire growth using the Haines Index. Weather and Forecasting 8, 223–234.
Westphal, D.L., Toon, O.B., 1991. Simulations of microphysical, radiative, and dynamic processes in a continental-scale forest-fire smoke plume. Journal of Geophysical Research: Atmospheres 96, 22379–22400.
Wiedinmyer, C., Akagi, S.K., Yokelson, R.J., Emmons, L.K., Al-Saadi, J.A., Orlando, J.J., Soja, A.J., 2011. The Fire INventory from NCAR (FINN): a high resolution global model to estimate the emissions from open burning. Geoscientific Model Development 4, 625–641.
Wilks, D.S., 2006. Statistical Methods in the Atmospheric Sciences, second ed. Academic Press.
Zhang, X., Kondragunta, S., Ram, J., Schmidt, C.C., Huang, H.-C., 2012. Near real time global biomass burning emissions product from geostationary satellite constellation. Journal of Geophysical Research: Atmospheres 117.
Zhang, X.Y., Kondragunta, S., Schmidt, C., Kogan, F., 2008. Near real time monitoring of biomass burning particulate emissions (PM2.5) across contiguous United States using multiple satellite instruments. Atmospheric Environment 42, 6959–6972.